Evolution of Surface Free Energy during Thin-Film Polymerization of Main-Chain Liquid Crystalline Polymers

Tai-Shung Chung* and Kui-Xiang Ma

Institute of Materials Research and Engineering, Department of Chemical Engineering, National University of Singapore, 10 Kent Ridge Crescent, Singapore 119260

Received: June 9, 1998; In Final Form: November 2, 1998

Through the use of a novel thin-film polymerization technique and the Lifshitz−van der Waals acid−base theory, we have determined, for the first time, the time evolution of contact angle and surface free energy during the polymerization (or molecular weight increase) of liquid crystalline poly(*p*-oxybenzoate/2,6-oxynaphthoate), poly(*p*-oxybenzoate), and poly(2,6-oxynaphthoate). Surface free-energy components of these main-chain liquid crystalline copolyesters and homopolyesters were calculated from contact angle measurements using a Ramé−Hart goniometer and three liquids (water, glycerol, and diiodomethane). Experimental data suggest that the Lewis base parameter, (γ^-) of poly(*p*-oxybenzoate/2,6-oxynaphthoate) decreases rapidly with polymerization progression, but the Lewis acid parameter (γ^+) and the Lifshitz−van der Waals parameter (γ^{LW}) do not vary significantly. The rapid decrease in the Lewis base parameter coincides with Fourier transform infrared spectra that indicate carboxyl and acetoxy peaks decreasing significantly in the early stages of a polycondensation reaction. In addition, since the activity of a naphthalene is less than that of a phenylene, an increase in naphthalene mole ratio in poly(*p*-oxybenzoate/2,6-oxynaphthoate) results in a decrease in the Lewis base parameter (γ^-) of copolymers. Furthermore, the poly(*p*-oxybenzoate) homopolymer exhibits higher surface free energy including the γ^+, γ^-, and γ^{LW} parameters than does the poly(2,6-oxynaphthoate) homopolymer. This study reconfirms our previous experimental report that the wholly aromatic main-chain liquid crystalline polymer poly(*p*-oxybenzoate/2,6-oxynaphthoate) with a 73/27 mole ratio has a monopolar Lewis base character because its γ^+ values were negligible. This conclusion can now be extended to this polymer with different mole ratios and to poly(*p*-oxybenzoate) and poly(2,6-oxynaphthoate) homopolymers.

1. Introduction

Thermotropic liquid crystalline polymers (LCPs) have attracted interest from both academia and industry because of their unique anisotropic mechanical properties, excellent chemical resistance, and high thermal stabilities. Several publications have described the scientific progress on this subject.[1−6] Currently, LCPs have two major applications: electronic devices and structural composites. However, the success of using LCPs for multilayer and miniature electronic devices depends on the surface free energy of LCPs and interfacial adhesion properties. To our knowledge, no one has ever published a work describing surface energy changes during the polymerization of main-chain thermotropic LCPs. The purpose of this work therefore, is to understand the mechanism of surface free-energy evolution during the thin-film polymerization of main-chain thermotropic LCPs.

Through the use of the monomer composition of Hoechst Celanese's liquid crystalline polyesters {for example, Vectra A-950 [a random copolymer of 73 mol % 4-hydroxybenzoic acid (HBA) and 27 mol % 6-hydroxy-2-naphthoic acid (HNA)]}, Geil and co-workers pioneered investigations into the microstructure of LCPs during polymerization using optical and transmission electron microscopy, X-ray studies, differential scanning calorimetry, and Fourier transform infrared (FTIR) spectroscopy.[7−10] A series of homopolymers and copolymers were synthesized using acetoxybenzoic acid (ABA) and 2,6-acetoxynaphthoic acid (ANA), which are acetylated from HBA and HNA, respectively.

Our research group has developed a novel thin-film polymerization technique for in situ examination and analysis of polycondensation reactions and liquid-crystal phase growth mechanisms of wholly aromatic LCPs, such as poly(ABA/ANA) copolymers and poly(ABA) and -(ANA) homopolymers.[11] In short, a thin layer of monomers was sandwiched between two glass slides with a steel ring as a spacer, and the thin-film polymerization was conducted on the heating stage of a microscope. The bottom slide contained a mixture of monomers that were solution-cast on the slide and dried. When the temperature reached a certain value, a sublimation (of monomers from bottom slide to upper slide)−recrystallization−melting−polymerization−LC domain formation−crystallization process occurred on the upper slide during the preparation of the polymer. The ring spacer provided space for easy removal or release of acetic acid during polymerization. Without the spacer, reproducibility was quite low and film quality was poor because the evaporation (or release) of acetic acid at elevated temperatures was vigorous. The progress of crystallization during the late stage of polymerization was found to be strongly dependent on the system morphology.

In this study, we intend to extend our previous technique to study the surface properties of LCPs during thin-film polymerization. To our surprise, only a few papers have been published on the surface energy of LCPs,[12−17] and most of them studied side-chain liquid crystalline polymers.[12−15] For example, Uzman

* To whom correspondence should be addressed. E-mail: chencts@nus.edu.sg. Fax: 65-7791936.

10.1021/jp982563r CCC: $18.00
Published on Web 12/15/1998

et al.[12] investigated surface tensions (γ) of branched polyethylene melts and two side-chain liquid-crystalline polyacrylate (LCPA) melts in isotropic, nematic, and smectic states using the pendant-drop method. The relationship between surface tension and temperature of LCPA melts showed abnormal behavior when compared with normal polymer melts, which only vary negatively and linearly with temperature. When LCPA was in its isotropic state, γ increased as the temperature decreased. This relationship changed near the isotropic−nematic transition. In the nematic state, γ again increased as the temperature decreased, until it reached the nematic−smectic transition, where γ jumped to higher values. Uzman et al. explained that these interesting phenomena were due to the fact that the mesogenic side groups governed the surface properties of LCPA.

Correia et al.[14] reported the surface tension of a side-chain liquid crystalline polyacrylate (poly{3-[4-(4-cyanophenyl)-phenoxy]propyloxycarbonyl}ethylene) which was provided by Merck. The γ was estimated from Neumann's equation, Owens and Wendt's equation (geometric-mean method), as well as Good and van Oss' equation (Lifshitz−van der Waals acid−base method) (LWAB), by measuring contact angles. They found γ values in the range of 40−45 mJ/m^2 from different approaches.

Chung and co-workers[16,17] were the first group to study the surface free energies of main-chain liquid crystalline polyesters (Vectra A-950 and Xydar SRT-900) and poly(ester−amide) (Vectra B-950). Various surface free-energy calculation approaches were employed to analyze the contact angle data. They found that surface free-energy values did match between two-liquid geometric-mean and three-liquid LWAB approaches if the correct combinations of testing liquids were used. However, the three-liquid LWAB provided more information, e.g., acidity and basicity of LCP surfaces.[17] They also reported that these LCP surface free energies could be theoretically estimated from the group contributions of their repeating unit.[16]

In this paper, we intend to combine our knowledge of thin-film polymerization and surface free energies to investigate the surface free-energy evolution during the polymerization reaction for the wholly aromatic polymers prepared from ABA and ANA.

2. Modern Acid−Base Theory

In the modern theory of surface science, Fowkes was the first to propose the theory of acid−base interfacial interaction.[18] The surface free energy here consists of two components: apolar (γ^d) interacts and acid−base (γ^{AB}) interactions. To determine the strengths of acidic and basic sites of polymers, Fowkes suggested using spectroscopic or calorimetric methods.

van Oss and Good[19−22] created two new parameters to redefine γ^{AB} interaction and quantify its strength: $\gamma^+ \equiv$ Lewis acid parameter of surface free energy and $\gamma^- \equiv$ Lewis base parameter of surface free energy.

$$\gamma^{AB} = 2\sqrt{\gamma^+\gamma^-} \tag{1}$$

On the basis of these definitions, a material is classified as a bipolar substance if both its γ^+ and its γ^- are greater than 0 ($\gamma_i^{AB} > 0$). In other words, it has both nonvanishing γ^+ and γ^-. instance, water is a typical bipolar substance. A monopolar material is one having either an acid or a base character, which means either $\gamma^+ = 0$ and $\gamma^- > 0$ or $\gamma^+ > 0$ and $\gamma^- = 0$. Chloroform is a monopolar acidic substance, and ether is a monopolar basic substance. An apolar material such as diiodomethane, is neither an acid nor a base (both its γ^+ and its γ^- are 0). For both monopolar and apolar materials, their $\gamma^{AB} = 0$.

van Oss and Good also expressed surface free energy as

$$\gamma = \gamma^{LW} + \gamma^{AB} = \gamma^{LW} + 2\sqrt{\gamma^+\gamma^-} \tag{2}$$

and

$$\gamma^{LW} = \gamma^d + \gamma^{dip} + \gamma^{ind} \tag{3}$$

where LW stands for Lifshitz−van der Waals, and the superscripts d, dip, and ind refer to (London) dispersion, (Keesom) dipole−dipole, and (Debye) induction, respectively. They have developed a "three-liquid procedure", and the following equation is used to determine γ_s using contact angle techniques and a traditional matrix scheme:

$$\begin{aligned}
\gamma_{L1}(1+\cos\theta_1) &= 2\left(\sqrt{\gamma_s^{LW}\gamma_{L1}^{LW}} + \sqrt{\gamma_s^+\gamma_{L1}^-} + \sqrt{\gamma_s^-\gamma_{L1}^+}\right)\\
\gamma_{L2}(1+\cos\theta_2) &= 2\left(\sqrt{\gamma_s^{LW}\gamma_{L2}^{LW}} + \sqrt{\gamma_s^+\gamma_{L2}^-} + \sqrt{\gamma_s^-\gamma_{L2}^+}\right)\\
\gamma_{L3}(1+\cos\theta_3) &= 2\left(\sqrt{\gamma_s^{LW}\gamma_{L3}^{LW}} + \sqrt{\gamma_s^+\gamma_{L3}^-} + \sqrt{\gamma_s^-\gamma_{L3}^+}\right)
\end{aligned} \tag{4}$$

In short, to determine the surface free energy, γ_s, of a polymer solid, three or more liquids were selected from the reference liquids table, two polar and one apolar.[23] Because the γ^{LW}, γ^+, and γ^- parameters of γ_{L1}, γ_{L2}, and γ_{L3} in eq 4 are available,[23] one can determine the γ^{LW}, γ^+, and γ^- parameters of γ_s by solving these three equations simultaneously together with the contact angle data. Hence, γ_s of the polymer solid can be obtained through eq 2.

3. Experiments

3.1. Preparation of ABA and ANA Monomers. The ABA and ANA monomers were prepared by acetylation of HBA and HNA separately, with acetic anhydride in refluxing toluene in the presence of a catalytic amount of pyridine. The reactions took 4 h to complete and were followed by recrystallization of ABA in butyl acetate and ANA in methanol, respectively. The success of monomer acetylation was confirmed by NMR.

3.2. Thin-Film Polymerization. ABA and ANA monomers with specific mole ratios were codissolved in acetone. The solution was then deposited onto microglass slides, and acetone evaporated in a few minutes. Another microglass slide was used to cover the one with the monomer and spaced about 0.5 mm apart by aluminum foil. The spacer provides the space or channel for the easy removal or release of acetic acid during polymerization. The whole set was then wrapped with aluminum foil and was heated at 270 °C ± 1% on a digital hot plate for 4, 8, 15, 30, 60, and 120 min, respectively. The whole package was removed from the thermostat hot stage immediately after its heating time and cooled under ambient temperature (~25 °C).

Similar to our previous description, the sample package in which the monomers were deposited on the bottom slide and sandwiched between two glass slides was chosen.[11] When the monomers were heated on the hot plate, they sublimated from the bottom slide and condensed onto the upper one. Microscopic studies on the surface of the upper slide suggested that this sublimation−condensation deposition on a glass slide could eliminate monomer impurities and benefit contact angle measurement. Once the monomers were sublimated and deposited upon the upper glass slide, polymerization reactions were carried out immediately on the upper slide. A polarizing light micro-

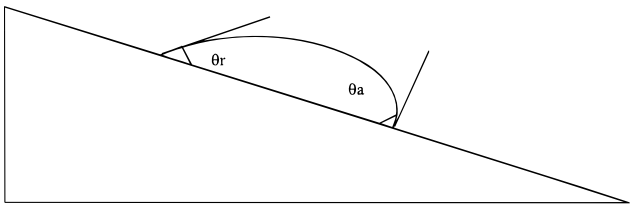

Figure 1. Liquid drop on a tilting base showing the advancing and receding contact angles.

TABLE 1. Surface Tension Parameters (mJ/m^2) of Testing Liquids

	water	glycerol	diiodomethane
γ^+	25.5	3.92	0.0
γ^-	25.5	57.4	0.0
γ^{AB}	51.0	30.0	0.0
γ^{LW}	21.8	34.0	50.8
γ	72.8	64.0	50.8

scope (Olympus BX50) was utilized to examine the sample morphology. Microscopy data suggest that sublimation occurs rapidly and the condensation reaction is a polymerization-controlled process.

3.3. FTIR Characterization. Samples with different reaction times were scratched from the upper glass slides, mixed with KBr, and molded for FTIR (Perkin-Elmer FTIR Spectrum 2000 Spectrometer) study.

3.4. Testing Liquids. Deionized water (prepared in this laboratory), glycerol (from BDH), and diiodomethane (from Nacalai Tesque) were chosen as the testing liquids because significant data are available for these liquids.[21,22] All were reagent grade and used as received. Table 1 tabulates their basic surface tension parameters (in mJ/m^2).

3.5. Contact Angle Measurements. The contact angle measurements were made on a Ramé−Hart contact angle goniometer (model 100-22) by the sessile drop method at 25 °C using an environmental chamber. A built-in image system provided by Ramé−Hart was able to acquire the image, transmit to a computer, and perform the image analysis. Liquid droplets were laid by a Gilmont microsyringe onto the surfaces of ABA/ANA thin-film polymerization samples (the upper glass slide).

Advancing and receding contact angles were obtained through a tilting base using the basic technique and principles developed elsewhere.[23,24] When a liquid drop resting on a solid surface is inclined, it deforms. The contact angle of the advancing edge of the drop increases while the angle of the receding edge decreases, as shown in Figure 1. The drop remains firmly adhered to the surface, stationary until the advancing (θ_a) and receding (θ_r) angles exceed certain critical volumes.

Normally, five droplets at different regions of the same piece of film were deposited, and two pieces of samples were used to get reliable contact angle data. Thus, 10 contact angles were averaged for each kind of sample, as well as each kind of testing liquid.

4. Results and Discussion

4.1. Hysteresis. To ensure that our contact angle data are reliable, we first studied the contact angle hysteresis. This is due to the fact that Young's equation for surface tension is derived by assuming a liquid in contact with an ideally homogeneous, smooth, and rigid solid. However, in practical conditions of wetting, the contact angle presents hysteretic character. Several reasons for this hysteresis have been evoked:[25−31] (1) diffusion of the liquid into the solid leading to swelling and local adsorption, (2) the orientation of macromolecular chains in the case of polymeric substrates, (3) drop size effects, and (4) most likely surface roughness and chemical heterogeneity.

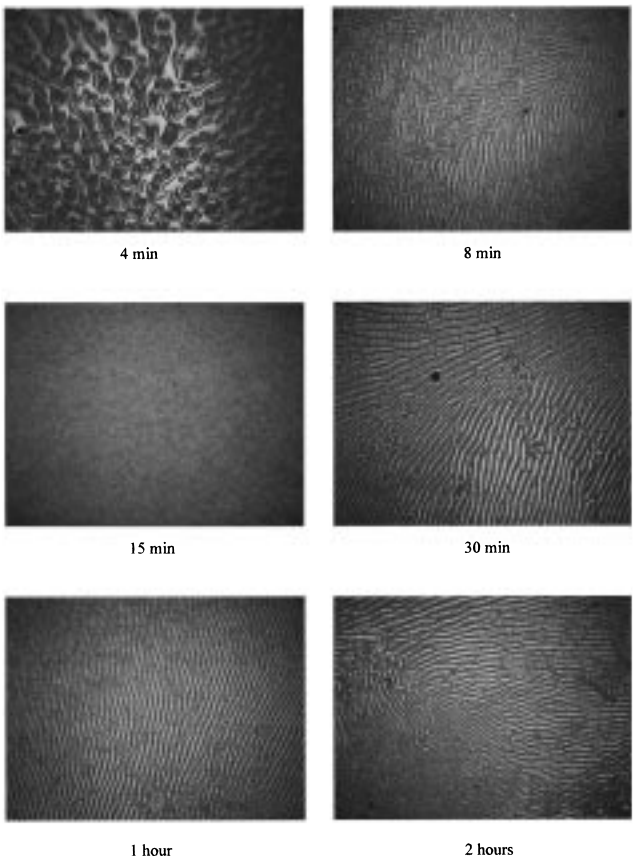

Figure 2. Morphology of ABA/ANA(50/50) copolymers under a ×40 optical microscope.

Drelich and co-workers[29−33] found that no contact angle change with respect to drop (bubble) size in the range of 1−7 mm was observed when smooth and homogeneous solid surfaces were prepared. However, for rough and/or heterogeneous surfaces, their contact angle measurements showed some specific features of the surfaces, such as (a) the contact angles were scattered, (b) contact angle hysteresis [the difference between the advancing and receding contact angles ($\theta_a - \theta_r$)] was large, (c) the advancing and receding contact angles differed because of the different techniques used (sessile-drop or captive-bubble), and (d) the variation of contact angle with drop (bubble) size was obvious.

For our ABA/ANA thin-film polymerization samples, there are some surface imperfections because of the polymerization, as well as the nature of liquid crystalline polymers. Figure 2 shows the morphologies of ABA/ANA copolymer (50/50 molar ratio) samples with different reaction times under a ×40 optical microscope. It is clear that striped liquid crystalline textures exist on the thin-film surfaces, which may cause the hysteresis.

However, the difference between the advancing and receding contact angles was found to be less than 10° for all of our samples, no matter if they were copolymers or homopolymers. In other words, the contact angle hysteresis is not very large compared to a 30° value as reported elsewhere.[24] Second, variations in advancing and receding contact angles with drop size are not very obvious in the range of 1−3 mm drop size diameter. Third, when the tilting base is flat, the right, and left-hand sides of the contact angles do not scatter much compared to the experimental error.[32] This strongly suggests that the local

TABLE 2. Contact Angles (deg) and Standard Deviations of 73/27 ABA/ANA Copolymers

	testing liquid		
angle	Water	glycerol	diiodomethane
ABA/ANA = 73/27; 270 °C Hot Plate, 4 min			
advancing	64.6 (2.9)	64.4 (1.6)	39.6 (2.1)
receding	59.6 (2.9)	57.6 (0.4)	34.6 (1.8)
ABA/ANA = 73/27; 270 °C Hot Plate, 8 min			
advancing	71.4 (2.8)	64.0 (0.8)	40.0 (1.9)
receding	66.6 (3.4)	57.4 (1.8)	35.0 (2.2)
ABA/ANA = 73/27; 270 °C Hot Plate, 15 min			
advancing	75.9 (2.1)	64.4 (0.8)	35.3 (0.9)
receding	71.4 (1.5)	58.0 (0.9)	29.9 (0.9)
ABA/ANA = 73/27; 270 °C Hot Plate, 30 min			
advancing	77.0 (0.9)	65.6 (1.1)	35.4 (1.9)
receding	72.1 (1.0)	59.0 (1.5)	30.2 (1.6)
ABA/ANA = 73/27; 270 °C Hot Plate, 60 min			
advancing	81.0 (1.1)	72.0 (1.9)	35.8 (1.8)
receding	74.8 (1.0)	64.3 (1.9)	29.2 (0.6)
ABA/ANA = 73/27; 270 °C Hot Plate, 120 min			
advancing	82.1 (1.3)	66.7 (1.8)	35.7 (2.1)
receding	77.0 (1.3)	59.5 (2.0)	31.0 (2.6)

difference in surface topography is limited. Finally, the roughness of ABA/ANA (50/50 molar ratio) copolymer samples with different polycondensation reaction times, from 4 to 120 min, was examined using an atomic force microscope and found to be very small compared to the drop size (approximately 1.5×10^{-5} vs 2−3 mm). Therefore, our thin-film polymerization samples on the upper microglass slides should be acceptable for contact angle measurements and surface free-energy calculations.

4.2. Contact Angle of ABA/ANA Copolymers. All of the advancing and receding contact angles and the standard deviations of the ABA/ANA copolymers with three different testing liquids and various reaction times are listed in Tables 2−4 for ABA/ANA monomer mole ratios of 73/27, 50/50, and 27/73, respectively.

For each of the testing liquids, each mole ratio of the copolymers, and each kind of reaction time, the difference between advancing and receding contact angles is less than 10° and, for most cases, the standard deviations are less than 2. On the basis of previous work,[29−31] it may be concluded that all of the copolymer surfaces obtained from thin-film polymerization have minor hysteresis but they are suitable for contact angle measurements.

Because the advancing contact angle more precisely represents the equilibrium contact angle than the receding angles,[21,26,29] only the advancing contact angles will be discussed hereafter. Table 2 shows the contact angles with the most polar liquid (water), the least polar liquid (glycerol), and the apolar liquid (diiodomethane) on 73/27 ABA/ANA copolymers under different reaction times. As expected, polar liquids give bigger contact angles than the apolar liquid. Moreover, it is quite obvious that the water contact angle increases with an increase in the reaction time, e.g., from 64° at 4 min to 82° at 120 min reaction time. However, it is interesting to see that both glycerol and diiodomethane contact angles do not vary significantly compared to water. Similar trends are also found in 50/50 and 27/73 ABA/ANA copolymers as shown in Tables 3 and 4, respectively. Water contact angles of 50/50 ABA/ANA copolymers increase from 67° at 4 min to 84° at 120 min reaction time whereas those of 27/73 ABA/ANA copolymers increase from 74° to 87° at 4 to 120 min reaction time. Clearly, with an increase in polymerization time, the polarity (in terms of Lewis acid and base interaction) of the copolymer surfaces decreases.

TABLE 3. Contact Angles and Standard Deviations of 50/50 ABA/ANA Copolymers

	testing liquid		
angle	water	glycerol	diiodomethane
ABA/ANA = 50/50; 270 °C Hot Plate, 4 min			
advancing	67.7 (1.6)	66.8 (0.5)	35.9 (2.2)
receding	63.4 (1.7)	62.0 (0.8)	29.4 (1.3)
ABA/ANA = 50/50; 270 °C Hot Plate, 8 min			
advancing	74.8 (1.3)	66.8 (1.4)	36.4 (1.1)
receding	70.4 (0.5)	61.3 (1.0)	27.4 (0.9)
ABA/ANA = 50/50; 270 °C Hot Plate, 15 min			
advancing	79.3 (1.2)	66.9 (2.0)	38.2 (0.2)
receding	74.0 (1.2)	59.5 (1.5)	32.8 (0.6)
ABA/ANA = 50/50; 270 °C Hot Plate, 30 min			
advancing	81.5 (1.0)	70.5 (0.4)	34.8 (1.3)
receding	76.3 (1.3)	63.4 (0.2)	28.0 (1.0)
ABA/ANA = 50/50; 270 °C Hot Plate, 60 min			
advancing	83.5 (1.0)	69.0 (2.4)	36.0 (2.8)
receding	77.3 (1.2)	61.8 (2.4)	29.2 (3.0)
ABA/ANA = 50/50; 270 °C Hot Plate, 120 min			
advancing	83.9 (1.6)	67.0 (1.6)	39.0 (0.4)
receding	76.8 (1.9)	58.5 (2.5)	34.6 (0.7)

TABLE 4. Contact Angles (deg) and Standard Deviations of 27/73 ABA/ANA Copolymers

	testing liquid		
angle	water	glycerol	diiodomethane
ABA/ANA = 27/73; 270 °C Hot Plate, 4 min			
advancing	74.7 (2.7)	68.0 (1.4)	30.6 (0.3)
receding	69.0 (2.3)	60.6 (2.0)	23.7 (1.0)
ABA/ANA = 27/73; 270 °C Hot Plate, 8 min			
advancing	83.7 (0.6)	69.0 (0.5)	32.2 (0.9)
receding	78.0 (0.5)	62.0 (1.4)	25.0 (0.8)
ABA/ANA = 27/73; 270 °C Hot Plate, 15 min			
advancing	84.6 (2.2)	70.3 (0.8)	35.5 (0.7)
receding	77.8 (2.2)	61.9 (1.4)	28.1 (1.6)
ABA/ANA = 27/73; 270 °C Hot Plate, 30 min			
advancing	86.6 (1.4)	71.3 (1.3)	33.4 (1.7)
receding	81.0 (1.5)	62.9 (1.6)	25.4 (2.4)
ABA/ANA = 27/73; 270 °C Hot Plate, 60 min			
advancing	87.5 (2.0)	72.3 (0.6)	33.8 (1.1)
receding	79.6 (2.8)	64.4 (1.6)	27.0 (1.4)
ABA/ANA = 27/73; 270 °C Hot Plate, 120 min			
advancing	87.4 (1.2)	71.0 (1.4)	32.2 (1.8)
receding	79.3 (2.7)	63.0 (0.9)	28.0 (2.4)

4.3. Surface Free Energy and Its Acid and Base Components of ABA/ANA Copolymers. To obtain surface free energies of ABA/ANA copolymers, van Oss and Good's three-liquid LWAB method is utilized. We chose diiodomethane as the apolar liquid and water−glycerol as the polar liquid pair. Table 5 shows the calculated results using eq 4.

There are three sections in Table 5. Part A tabulates all of the surface free-energy components (γ^+, γ^-, γ^{AB}, and γ^{LW}), as well as the total surface free energy (γ) of 73/27 ABA/ANA copolymers under different reaction times. Similarly, the surface free energy and its components of 50/50 and 27/73 ABA/ANA copolymers are tabulated under parts B and C, respectively.

In all three parts, the Lewis acid parameters (γ^+) of all three ratios of the ABA/ANA copolymers are very small, varying from 0 to 0.2 mJ/m^2, resulting in quite small acid−base parameters ($\gamma^{AB} = 2\sqrt{\gamma^+\gamma^-}$). Moreover, for each ratio of the ABA/ANA copolymers, the Lifshitz−van der Waals parameters (γ^{LW}) do not vary much with the reaction time. γ^{LW} is in the range of 39.6−41.8 mJ/m^2 for 73/27 ABA/ANA copolymers synthesized from different reaction times, 40.1−42.1 mJ/m^2 for

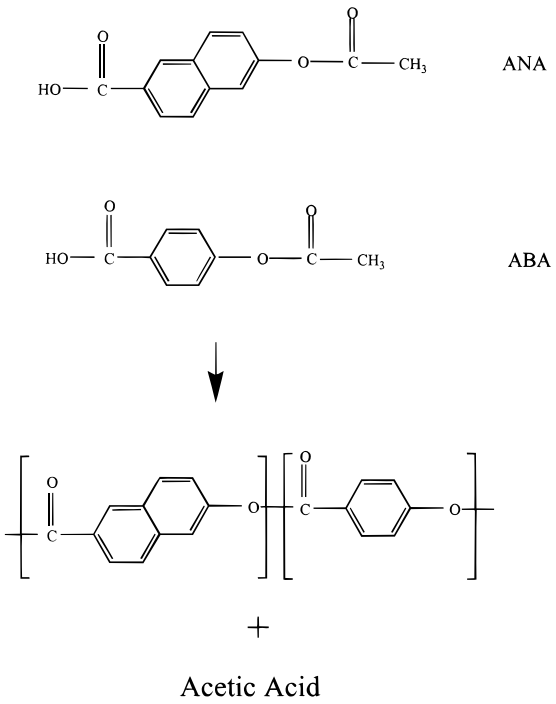

Figure 3. Monomer structures and polymerization formulation.

TABLE 5. Surface Free-Energy Components of ABA/ANA Copolymers (Calculated with the three-Liquid LWAB Method)

copolymer	reaction time (min)	surface free-energy component (mJ/m^2) γ^+	γ^-	γ^{AB}	γ^{LW}	γ
(A) ABA/ANA = 73/27	4	0.00	19.71	0.28	39.79	40.07
	8	0.13	11.08	2.42	39.63	42.05
	15	0.15	6.69	2.03	41.87	43.90
	30	0.11	6.28	1.68	41.85	43.53
	60	0.00	6.00	0.00	41.68	41.68
	120	0.21	3.12	1.63	41.71	43.34
(B) ABA/ANA = 50/50	4	0.00	17.16	0.00	41.59	41.59
	8	0.02	9.02	0.89	41.36	42.25
	15	0.15	5.18	1.78	40.48	42.26
	30	0.00	4.92	0.24	42.13	42.38
	60	0.10	3.04	1.12	41.56	42.69
	120	0.26	2.60	1.64	40.12	41.76
(C) ABA/ANA = 27/73	4	0.00	9.47	0.00	44.00	44.00
	8	0.05	2.85	0.78	43.27	44.05
	15	0.06	2.82	0.79	41.78	42.57
	30	0.03	1.99	0.50	42.76	43.26
	60	0.02	1.84	0.35	42.56	42.92
	120	0.05	1.55	0.53	43.28	43.81

50/50 ABA/ANA, and 41.8−44.0 mJ/m^2 for 27/73 ABA/ANA copolymers, respectively.

However, the Lewis base parameters (γ^-) are absolutely and monotonically decreasing with an increase in the reaction time for all copolymers. γ^- decreases dramatically from 19.71 mJ/m^2 at 4 min to 3.12 mJ/m^2 at 120 min reaction time for 73/27 ABA/ANA copolymers. Similarly, for 50/50 ratio and 27/73 ratio copolymers, γ^- decreases from 17.16 mJ/m^2 for 4 min to 2.60 mJ/m^2 for 120 min reaction time and from 9.47 mJ/m^2 for 4 min to 1.55 mJ/m^2 for 120 min reaction time, respectively. In other words, the strength of the Lewis base parameter decreases with the progression of ABA/ANA copolymerization. Figure 3 shows the monomer structures as well as the copolymerization formulation. With the progression of polymerization, more acetoxy and carboxyl groups combine to release the acetic acid; therefore, the decrease of γ^- of the surface is understandable.

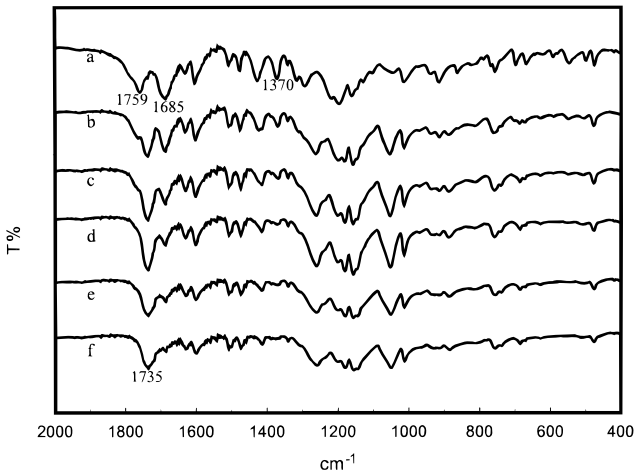

Figure 4. FTIR spectra obtained by 73/27 ABA/ANA copolymers at different reaction times: (a) 4. (b) 8, (c) 15, (d) 30, (e) 60, and (f) 120 min.

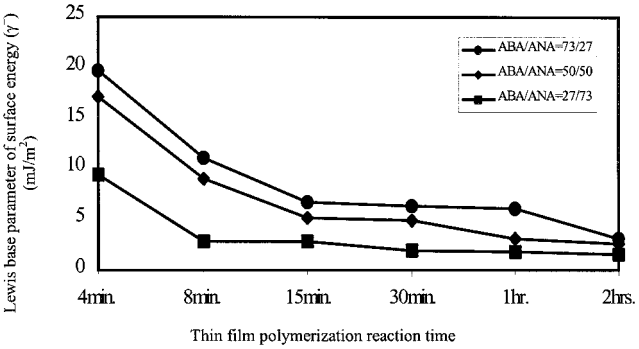

Figure 5. Lewis base parameter of surface energy of copolymers with different monomer ratios.

Figure 4 shows the FTIR spectra of the thin-film 73/27 ABA/ANA copolymer as a function of the reaction time varying from 4 to 120 min. Generally, the peak at 1685 cm^{-1} is the vibration of the C═O bond in carboxyl, the peak at 1370 cm^{-1} is the C−H bond in acetoxy, and the peak at 1759 cm^{-1} is the C═O bond in acetoxy. Moreover, the peak at 1735−1740 cm^{-1} is the C═O bond in polymer ester. It is clear that the peaks of both the carboxyl and the acetoxy groups are decreasing while the peak of polymer ester is increasing with an increase in the reaction time. At the end of the reaction, as shown in the spectrum in Figure 5f, the peaks at 1370, 1685, and 1759 cm^{-1} are almost indistinguishable compared to their original height, which indicates that nearly all of the acetoxy and carboxyl groups have been consumed. Meanwhile, a substantial number of polymer ester groups have formed as shown by the increment of the peak at 1735−1740 cm^{-1}. Moreover, it is obvious that the condensation polymerization is much faster in the beginning stage (e.g., from 4 to 15 min) than in the later stage (e.g., from 30 to 120 min) because both carboxyl and acetoxy peaks decrease significantly from 4 to 15 min. These results coincide with and explain well the trend of the Lewis base parameter (γ^-) shown in part A of Table 5, where γ^- decreases far more from 4 to 15 min reaction time than from 30 to 120 min reaction time.

Table 6 compares the surface free-energy components of the 73/27 ABA/ANA copolymer at 120 min with those of commercial grade Vectra A-950,[17] which contains the same mole ratio of monomers. The table shows that all of the surface free-energy components between our thin-film copolymer and Vectra A-950 are quite close. This excellent agreement strongly

TABLE 6. Surface Free-Energy Comparisons between 73/27 ABA/ANA Thin-Film Copolymer and Vectra A-950 Spin-Coating Film

	polymerization time (min)	surface free-energy component (mJ/m^2)				
		γ^+	γ^-	γ^{AB}	γ^{LW}	γ
copolymer	120	0.21	3.12	1.63	41.71	43.34
Vectra A-950	commercial	0.15	4.00	1.53	40.27	41.80

TABLE 7. Contact Angles (deg) and Standard Deviation of Poly(ABA) and -(ANA) Homopolymers

	liquid		
angle	water	glycerol	diiodomethane
Poly(ABA) Homopolymer with 120 min Reaction			
advancing	73.5 (2.4)	63.0 (2.5)	27.5 (1.7)
receding	69.0 (2.4)	57.4 (2.8)	18.0 (2.0)
Poly(ANA) Homopolymer with 120 min Reaction			
advancing	90.7 (2.2)	78.1 (1.6)	39.7 (2.4)
receding	83.4 (2.1)	70.7 (1.5)	33.7 (2.7)

TABLE 8. Surface Free-Energy Components of Poly(ABA) and -(ANA) Homopolymers

	polymerization time (min)	surface free-energy component (mJ/m^2)				
		γ^+	γ^-	γ^{AB}	γ^{LW}	γ
poly(ABA)	120	0.06	7.86	1.32	45.21	46.53
poly(ANA)	120	0.00	2.02	0.00	39.78	39.78

supports our previous hypothesis that the thin-film polymerization samples developed in this work are well-suited for contact angle measurements and the surface free-energy calculation. In addition, this excellent agreement also suggests that the absorption of acetic acid vapor by the thin film during polymerization at elevated temperatures can be negligible.

In addition, the current data reconfirm our conclusions in the previous papers[16,17] that Vectra A-950 has a monopolar Lewis base surface because its γ^+ values are negligible, which is consistent with van Oss and Good conclusion that ester has Lewis base character. This conclusion can also be extended to ABA/ANA copolymers obtained by thin-film polymerization with 73/27, 50/50, and 27/73 mole ratios with different polymerization times.

4.4. Effect of ANA Mole Ratio on the Surface Free Energy of LC Copolymers. *4.4.1. Lewis Base Parameters of Surface Free Energy.* Figure 5 not only shows the Lewis base parameter (γ^-) of ABA/ANA copolymers decreasing with an increase in reaction time, but it also shows an increase in the ANA ratio resulting in a decrease in the Lewis base parameter (γ^-). The only difference between ABA and ANA is that the phenylene unit in ABA is replaced by the naphthalene unit in ANA. Because the activity of naphthalene is less than that of phenylene, an increase in the mole ratio of naphthalene (ANA) in copolymers should decrease the overall Lewis base parameter (γ^-) (e.g., the acid−base property), as presented in this figure.

4.4.2. Surface Free Energy of Poly(ABA) and -(ANA) Homopolymers. For comparison and further understanding of the effect of ANA on surface free-energy properties, poly(ABA) and -(ANA) homopolymer samples are prepared by the same thin-film polymerization method (270 °C hot plate for 120 min). Table 7 summarizes their contact angle results, and Table 8 tabulates their surface free-energy components. Interestingly, the contact angles of all three testing liquids (e.g., water, glycerol, and diiodomethane) on poly(ANA) surfaces are much higher than those on poly(ABA) surfaces, and hence, poly(ABA) exhibits a higher surface free energy than poly(ANA). As shown in Table 8, the γ^-'s of both poly(ABA) and -(ANA) are much larger than the γ^+'s, which again indicates that these homopolymers should be classified as Lewis base materials as well. The γ^- and γ^{LW} of poly(ANA) are much lower than those of poly(ABA), which strongly reconfirms our previous conclusion that the substitution of phenylene (ABA) units by naphthalene (ANA) units lowers the acid−base property (represented by the Lewis base γ^- in our case) as well as the apolar property (γ^{LW}) of LCPs.

5. Conclusion

A novel thin-film polymerization technique and the Lifshitz−van der Waals acid−base theory were utilized to investigate acid−base interactions of wholly aromatic liquid crystalline poly(ABA/ANA) copolymers and poly(ABA) and -(ANA) homopolymers with different mole ratios as a function of polymerization time. Surface free-energy components of these liquid crystalline copolymers and homopolymers were calculated from the contact angle measurements using a Ramé−Hart goniometer with the three-liquid acid−base approach. Experimental data showed that the Lewis acid parameter (γ^+) and the Lifshitz−van der Waals parameter (γ^{LW}) of copolymers do not vary significantly with the progression of the polycondensation reaction, but the Lewis base parameters (γ^-) decrease rapidly. FTIR spectra revealed that the cause of the decreases in Lewis base parameters (γ^-) probably was due to the combining of acetoxy with carboxyl function groups which release acetic acid during the polymerization. We also found that an increase in the naphthalene mole ratio in poly(*p*-oxybenzoate/2,6-oxynaphthoate) resulted in a decrease in the Lewis base parameter (γ^-) of copolymers and that the poly(*p*-oxybenzoate) homopolymer exhibits higher surface free energies, including γ^+, γ^-, and γ^{LW}, than those of the poly(2,6-oxynaphthoate) homopolymer.

Furthermore, this study reconfirmed our previous experimental results that the wholly aromatic main-chain liquid crystalline polymer, 73/27 poly(*p*-oxybenzoate/2,6-oxynaphthoate), has a monopolar Lewis base character because its γ^+ values were negligible, which was consistent with van Oss and Good's conclusion that ester has Lewis base properties. The conclusion can now be extended to ABA/ANA copolymers with different mole ratios, as well as to poly(ABA) and -(ANA) homopolymers.

Acknowledgment. The authors are grateful to the Institute of Materials Research and Engineering (IMRE), Singapore, for financial support and the National University of Singapore (NUS) for the Research Fund No. RP 950696. Special thanks go to Miss Sixue Cheng for her useful technical help and Dr. S. Mullick for providing the monomers. Thanks are also due to Dr. Y. Lin, Mdm. L. K. Leong at IMRE, and Prof. R. J. Good at SUNY at Buffalo for their help and comments and Dr. J. Drelich at Michigan Technology U. for sending useful preprints.

References and Notes

(1) Calundann, G. W.; Jaffe, M. In Synthetic Polymers *Proceedings of the Robert A. Welch Found. Conf. Chem. Res.*; Houston, TX, 1982; p 297.

(2) Chung, T. S. *Polym. Eng. Sci.* **1986**, *26*, 901.

(3) Chung, T. S.; Calundann, G. W.; East, A. J. *Encyclopedia of Engineering Materials*; Marcel Dekker: 1989; Vol. 2, p 625.

(4) Jaffe, M.; Calundann, G. W.; Yoon, H. N. *Encyclopaedia of Fibre Science and Technology*; 1989; Vol. 3, p 83.

(5) Weiss, R. A.; Ober, C. K. *Am. Chem. Soc.* **1990**.

(6) Handlos, A. A.; Baird, D. G. *J. Macromol. Sci., Rev. Macromol. Chem. Phys.* **1995**, *C35*, 183.

(7) Rybnikar, F.; Yuan, B. L.; Geil, P. H. *Polymer* **1994**, *35*, 1863.

(8) Liu, J.; Rybnikar, F.; Geil, P. H. *J. Polym. Sci.; Part B: Polym. Phys.* **1992**, *30*, 1469.

(9) Rybnikar, F.; Yuan, B. L.; Geil, P. H. *Polymer* **1994**, *35*, 1831.
(10) Liu, J.; Rybnikar, F.; Geil, P. H. *J. Macromol. Sci., Phys.* **1996**, *b35*, 375.
(11) Cheng, S.; Chung, T. S.; Mullick, S. *Chem. Eng. Sci.* **1998**, in press.
(12) Uzman, M.; Song, B.; Runke, T.; Cackovic, H.; Springer, J. *Makromol. Chem.* **1991**, *192*, 1129.
(13) Runke, T.; Song, B.; Springer, J. *Ber. Bunsen-Ges. Phys. Chem.* **1994**, *98*, 508.
(14) Correia, N. T.; Ramos, J. J.; Saramago, M. B. J. V.; Calado, J. C. G. *J. Colloid Interface Sci.* **1997**, *189*, 361.
(15) Wang, J.; Mao, G.; Ober, C. K.; Kramer, E. *Macromolecules* **1997**, *30*, 1906.
(16) Chung, T. S.; Ma, K. X.; Jaffe, M. *Macromol. Chem. Phys.* **1998**, *199*, 1013.
(17) Ma, K. X.; Chung, T. S.; Good, R. J. *J. Polym. Sci. Phys.* **1998**; in press.
(18) Fowkes, F. M. *J. Adhes. Sci. Technol.* **1987**, *1*, 7.
(19) van Oss, C. J.; Ju, L.; Chaudhury, M. K.; Good, R. J. *J. Colloid Interface Sci.* **1989**, *128*, 313.
(20) van Oss, C. J.; Chaudhury, M. K.; Good, R. J. *Chem. Rev.* **1988**, *88*, 927.
(21) Good, R. J.; van Oss, C. J. *Modern Approaches to Wettability*; Plenum: New York, 1991; p 1.
(22) Good, R. J. *Contact Angle, Wetting, and Adhesion*; VSP: Utrecht, The Netherlands; 1993; p 3.
(23) MacDougall, G.; Okrent, C. *Proc. R. Soc. London, Ser. A* **1942**, *180*, 151.
(24) Extrand, C. W.; Kumagai, Y. *J. Colloid Interface Sci.* **1996**, *184*, 191.
(25) Marmur, A. *Colloids Surf., A* **1996**, *116*, 55.
(26) Good, R. J. *Surface Colloid and Science II: Experimental Methods*; Plenum: New York, 1979; Chapter 1.
(27) Herzberg, W. J.; Marian, J. E. *J. Colloid Interface Sci.* **1970**, *33*, 161.
(28) Herzberg, W. J.; Marian, J. E.; Vermeulen, T. *J. Colloid Interface Sci.* **1970**, *33*, 164.
(29) Drelich, J.; Miller, J. D.; Good, R. J. *J. Colloid Interface Sci.* **1996**, *179*, 37.
(30) Drelich, J.; Miller, J. D.; Kumar, A.; Whitesides, G. M. *Colloids Surf., A* **1994**, *93*, 1.
(31) Drelich, J.; Miller, J. D. *J. Colloid Interface Sci.* **1994**, *164*, 252.
(32) Drelich, J.; Laskowski, J. S.; Pawlik, M.; Veeramasuneni, S. *J. Adhes. Sci. Technol.* **1997**, *11*, 1399.
(33) Drelich, J. *Pol. J. Chem.* **1997**, *71*, 525.